Kinetic and thermodynamic resolution of the interactions between sulphite and the penta-heme cytochrome, NrfA, from Escherichia coli.

Gemma L Kemp, Thomas A Clarke, Sophie J Marritt, Colin Lockwood, Susannah R Poock, Andrew M Hemmings, David J Richardson, Myles Cheesman, Julea N Butt

KINETIC AND THERMODYNAMIC RESOLUTION OF THE INTERACTIONS BETWEEN SULPHITE AND THE PENTA-HEME CYTOCHROME, NrfA, FROM *ESCHERICHIA COLI*.

Gemma L. Kemp[*], Thomas A. Clarke[†], Sophie J. Marritt[*], Colin Lockwood[†], Susannah R. Poock[†], Andrew M. Hemmings[*,†], David J. Richardson[†], Myles R. Cheesman[*], Julea N. Butt[*,†]

From the Centre for Molecular and Structural Biochemistry, School of Chemistry[*] and School of Biological Sciences[†], University of East Anglia, Norwich Research Park, Norwich, NR4 7TJ, U.K.

Running head: NrfA and sulphite

Address correspondence to: Julea Butt, School of Chemistry, University of East Anglia, Norwich Research Park, Norwich, NR4 7TJ, U.K. Fax: +44 (0)1603 592003: E-mail: j.butt@uea.ac.uk.

Keywords: Protein film voltammetry, electron paramagnetic resonance, magnetic circular dichroism, nitrogen cycle, cytochrome, nitrite reductase.

Abbreviations

EPR, electron paramagnetic resonance; Hepes, 4-(2-hydroxyethyl)-1-piperazineethanesulfonic acid; MCD, magnetic circular dichroism; NrfA, penta-heme cytochrome *c* nitrite reductase; PFV, protein film voltammetry; SHE, standard hydrogen electrode.

Abstract

NrfA is a pentaheme cytochrome present in a wide-range of γ-, δ- and ε-proteobacteria. Its nitrite and nitric oxide reductase activities have been studied extensively and contribute to respiratory nitrite ammonification and nitric oxide detoxification respectively. Sulphite is a third substrate for NrfA that may be encountered in the microoxic environments where *nrfA* is expressed. Consequently, we have performed quantitative kinetic and thermodynamic studies of the interactions between sulphite and *E. coli* NrfA to provide a biochemical framework from which to consider their possible cellular consequences. A combination of voltammetric, spectroscopic and crystallographic analyses define dissociation constants for sulphite binding to NrfA in oxidised (ca. 54 μM), semi-reduced (ca. 145 μM) and reduced (ca. 180 μM) states that are comparable to each other and to the K_M (ca. 70 μM) for sulphite reduction at pH 7. Under comparable conditions K_M values of ca. 22 and 300 μM describe nitrite and nitric oxide reduction respectively, while the affinities of nitrate and thiocyanate for NrfA drop more than 50-fold on enzyme reduction. These results are discussed in terms of the nature of sulphite coordination within the active site of NrfA and their implications for the cellular activity of NrfA.

INTRODUCTION

The pentaheme cytochrome NrfA was first identified in the enteric pathogen *Escherichia coli* where its role in anaerobic nitrate respiration is now well-established. At low nitrate concentrations expression of *napABC* and *nrfABCD* allows quinol oxidation to be coupled to the periplasmic reduction of, respectively, nitrate to nitrite and nitrite to ammonium. In themselves these reactions are not proton motive. However, they contribute to maintaining a trans-membrane proton gradient by regenerating the quinone required for the proton-motive oxidation of formate by formate dehydrogenase-N. NrfA contributes to this process by catalysing the six-electron reduction of nitrite to ammonium and homologues have been identified in a wide range of γ-, δ- and ε-proteobacteria that have environmental, medical and biotechnological importance [1].

Enzymes of the NrfA family have a high degree of sequence similarity and this is reflected in their highly conserved three dimensional structures [2-5]. Four *bis*-histidine coordinated *c*-hemes form two branches that converge on the active site from distinct areas on the surface of the enzyme. The active site pocket is defined by the side-chains of conserved histidine, tyrosine and arginine residues together with the distal face of a *c*-heme having lysine as its proximal ligand. A crystal structure of *Wolinella succinogenes* NrfA shows nitrite coordinated to the distal face of the active site heme through its N-atom and with its oxygens hydrogen-bonded to histidine and arginine [6]. These residues together with tyrosine may facilitate catalysis by delivering the protons needed for the reductive transformation of nitrite to ammonium; $NO_2^- + 6e^- + 8H^+ \rightarrow NH_4^+ + 2H_2O$.

NrfA also catalyses the reduction of nitric oxide to ammonium [7-9]. Nitric oxide is cytotoxic and the presence of NrfA has been shown to contribute to defence against exogenous nitric oxide in *Salmonella typhimurium* and *Escherichia coli* [10, 11]. Thus, NrfA has the capacity to contribute to both respiration and detoxification as necessitated by the prevailing conditions and some insight into the likely activity of NrfA in the presence of both nitric oxide and nitrite is provided by the steady-state kinetic parameters for these reductions. For *E. coli* NrfA a combination of protein film voltammetry (PFV) and spectrophotometric analyses has defined values of k_{cat} and K_M for nitric oxide reduction of ca. 840 s^{-1} and 300 μM, respectively, at pH 7 [8]. Nitrite reduction occurs with a k_{cat} ~770 s^{-1} and K_M ~ 30 μM under comparable conditions [8, 12]. It is likely that both nitrite and nitric oxide bind as distal ligands to the active site heme prior to their reduction. Certainly similar electrochemical potentials are required to observe appreciable activity towards both substrates which is consistent with their reduction at a common site. Thus, at neutral pH, if the levels of NrfA in the cell are such that the enzyme can be saturated with the nitrogenous substrates, high levels of nitric oxide relative to nitrite will be required to favour nitric oxide detoxification over nitrite respiration.

A third substrate of NrfA is sulphite[1] [3, 7, 13, 14]. An essential nutrient and metabolite that may be present at high levels in microaerobic aquatic niches, sulphite is also cytotoxic. It is produced by neutrophils as part of host defence against microbial invasion and added to certain food and beverages as an antimicrobial [15, 16]. Consequently, NrfA may well encounter sulphite in a cellular context. Sulphite reduction by NrfA generates sulphide in a six-electron process that appears to parallel nitrite ammonification although the reaction pathway, and indeed the physiological role of this reaction, are presently unclear [13]. Steady-state parameters describing NrfA sulphite reduction that may inform on the possible cellular consequences of interactions between sulphite and NrfA have not been reported to date. However, where rates of sulphite reduction are documented they are at least as high as those of dedicated sulphite reductases although several orders of magnitude less than those for nitrite reduction under comparable conditions. It may also be significant that SO_3^{2-} (HSO_3^-) can bind as the distal ligand to the active site heme of *W. succinogenes* NrfA [13]. This suggests that sulphite will compete with nitrite and nitric oxide for binding to NrfA and, since it is reduced considerably more slowly than those substrates, its presence may have a significant impact on the rates of reduction of the nitrogenous substrates. In this context we have performed quantitative kinetic and thermodynamic studies to provide greater insight into the interactions between sulphite and *E. coli* NrfA in multiple oxidation states. Our results provide a detailed biochemical framework describing the interactions between a redox enzyme and its substrate and one from which the possible cellular consequences of these interactions can be considered.

EXPERIMENTAL

Materials

NrfA was purified from *E. coli* strain LCB2048 as previously described and concentrations were determined using ε_{410nm} = 497650 M^{-1} cm^{-1} for the oxidised enzyme [4, 17]. Unless stated otherwise experiments were performed in 50 mM Hepes, 2 mM $CaCl_2$, pH 7.0, 20 °C prepared with water of resistivity of >18 MΩ cm (Purelab Maxima, Elga) or 'Trace Select Ultra Water' (Fluka with ≤1 μg nitrite kg^{-1}). Fresh $NaNO_2$ and Na_2SO_3 stock solutions (pH 7.0) were prepared daily as required.

Protein film voltammetry

All potentials are quoted versus the Standard Hydrogen Electrode (S.H.E.) after adding 0.197 V to the value measured with a Ag/AgCl (saturated KCl) reference electrode. The experimental arrangement, in addition to data collection and analysis, were essentially as described previously [12, 18]. Briefly, pyrolytic graphite 'edge' working electrodes were coated with NrfA and rapidly rotated during experiments performed in N_2-filled chambers. Sulphite concentrations above 1 mM were avoided because currents arising from electrodic

[1] For simplicity in the text below we use the term 'sulphite' to encompass the species SO_3^{2-}, HSO_2^- and SO_2 that are formed in a pH-dependent equilibrium when Na_2SO_3 dissolves in aqueous solution.

sulphite reduction interfered with accurate assessment of the currents arising from NrfA dependent processes.

The Michaelis constant (K_M) and maximum catalytic current (i_{max}) describing NrfA nitrite reduction in a solution of defined sulphite concentration were determined from the catalytic currents measured by chronoamperometry in response to titrating nitrite into the sample. Before fitting these currents to the Michaelis-Menten equation, they were corrected for first order loss of magnitude over time and Koutecky-Levich analysis used as appropriate to determine the response at infinitely high rotation rates, i.e., in the absence of mass-transport limitations. Where it was necessary to compare results from different films this was done after normalizing the response of each film to that recorded during cyclic voltammetry at 30 mV s^{-1}, 3000 rpm in 5 μM nitrite.

For competitive inhibition, the dissociation constant, K_d, describing binding of the inhibitor, I, to the enzyme was determined from the equation: $K_M = K_M^0\left(1+[I]/K_d\right)$, where K_M^0 is the Michaelis constant in the absence of inhibitor. For mixed inhibition, values for the dissociation constants K_d^R and $K_d^{R:Nitrite}$ describing inhibitor binding to the enzyme and enzyme:nitrite complex respectively were determined from the equation:

$\frac{1}{i_{max}} = \frac{1}{i_{max}^0}\left(\left(1+\frac{[I]}{K_d^R}\right)\Big/\left(1+\frac{[I]}{K_d^{R:Nitrite}}\right)\right)$, where i_{max}^0 is the maximum catalytic current in the absence of the inhibitor [19]. We note that the major conclusions drawn from the data are not changed by linear analysis of both the $1/i_{max}$ and K_M/i_{max} versus [I] plots that yields K_d^R ~ 87 μM and $K_d^{R:Nitrite}$ ~ 1270 μM.

Spectroscopic assessment of sulphite binding to NrfA

Sulphite binding to NrfA was monitored by X-band electron paramagnetic resonance (EPR), magnetic circular dichroism (MCD) and electronic absorption spectroscopies [4]. Values for the dissociation constant (K_d^O) describing sulphite binding to oxidised NrfA were determined from the variation of signal intensity with sulphite concentration fit to the equation describing reversible binding of a single molecule of sulphite to a single molecule of NrfA:

$$\frac{[\text{NrfA}:\text{sulfite}]}{[\text{NrfA}]_{total}} = \frac{\left(C-\sqrt{C^2-4[\text{NrfA}]_{total}[\text{sulfite}]_{total}}\right)}{2},$$

where [NrfA:sulphite] is the equilibrium concentration of the complex formed between NrfA and sulphite, $[NrfA]_{total}$ and $[sulphite]_{total}$ are the total concentrations of NrfA and sulphite respectively, and $C = [NrfA]_{total} + [sulphite]_{total} + K_d^O$. The concentration of NrfA:sulphite in the MCD sample was calculated using $\varepsilon_{532\ nm}$ = 53210 M^{-1} cm^{-1} since electronic absorption spectroscopy showed that both oxidised NrfA and its complex with sulphite had the same absorbance at this wavelength (supplemental Figure S1).

Crystallization, X-ray data collection, structure solution and refinement

NrfA was crystallized under the conditions previously reported [17]. A single crystal was soaked in the crystallization reservoir solution plus 50 mM $Na_2S_2O_5$ for 10 minutes at 277 K prior to transfer to a similar solution supplemented with both 50 mM $Na_2S_2O_5$ and 20% (v/v) ethylene glycol as cryoprotectant. X-ray diffraction from a single crystal maintained at 100 K was measured using an ASDC Q4 detector on beamline ID14.2 at the ESRF, Grenoble. The crystal was of space group $P2_1$ with cell dimensions a = 90.5 Å, b = 82.2 Å, c = 142.2 Å and β= 101.1°. Diffraction data were obtained to a resolution of 2.3 Å using X-rays at a wavelength of 0.933 Å. Microspectrophotometry established that exposure to X-rays was accompanied by photo-reduction of the NrfA hemes (supplemental Figure S1). This reduction appeared complete within 100 s of X-ray exposure. Consequently, to avoid combining data from both oxidised and reduced states of NrfA, only those images collected after 100 s of cumulative X-ray exposure, i.e., those arising from reduced NrfA, were processed using MOSFLM and integrated using SCALA as part of the CCP4 crystallography package [20-22]. A summary of data collection statistics is provided (supplemental Table S1).

The structure of sulphite-bound NrfA was determined by molecular replacement with MOLREP [22] employing a single monomer from the 1.7 Å resolution NrfA structure available in the Protein Data Bank (PDB entry, 2RDZ) as a search model [23]. This revealed four monomers of NrfA in the crystallographic asymmetric unit. This model was refined using several rounds of manual building using COOT [24] and automatic refinement using REFMAC [25]. Addition of 957 water molecules using ARP [26] and COOT, as well as eight sulphite molecules and twelve ethylene glycol molecules gave a final structure with a final R_{cryst} (R_{free}) of 17.7 (23.8) for data in the range 50.4 – 2.3 Å. When analysed using MOLPROBITY [27], 1756 residues in the unit cell were in the allowed regions, with four residues in unfavoured regions being the histidines of the active sites. The refined coordinates have been deposited in the Protein Databank with accession number 3L1T.

Assays of sulphite reduction

Steady-state rates of sulphite reduction were measured in a spectrophotometric assay through the NrfA (0.3 μM) dependent oxidation of Zn reduced methyl viologen (1 mM) in anaerobic 50 mM Hepes, 2 mM $CaCl_2$, 5 mM EDTA, pH 7.0 that contained the desired concentration of sulphite [17]. To verify sulphide as the product of sulphite reduction, NrfA and dithionite were incubated in N_2-sparged sealed cuvettes. Dithionite oxidation was quantified using ε_{315nm} = 8 mM^{-1} cm^{-1} for $S_2O_4^{2-}$ [28] and sulphide determined colorimetrically by the method of Cline [29].

Construction of an *E. coli nrfA* deletion strain and assessment of the impact of sulphite on anaerobic growth

The phage λ Red recombinase PCR mutagenesis system was used to delete *nrfA* from *E. coli* strain DH10B [30, 31]. Primers were designed to generate a PCR product consisting of the kanamycin resistance gene from pKD13 flanked by regions homologous to nucleotides adjacent to *nrfA*. This PCR product was used to electro-transform *E. coli* DH10B expressing the λ Red recombinase via the arabinose-inducible plasmid pKD46. A kanamycin resistant transformant was then selected and the chromosomal mutation verified by colony PCR. To confirm the expected phenotype periplasmic extracts were prepared from cultures of the *nrfA* deletion strain and DH10B after overnight anaerobic growth in glycerol/nitrate/fumarate medium for optimal *nrfA* expression [17]. The extract from DH10B, but not that from the *nrfA* deletion strain displayed nitrite reductase activity in a spectrophotometric assay using dithionite reduced methyl viologen as the electron donor and a heme-staining band of ca. 50 kDa corresponding to NrfA when resolved by SDS-PAGE [31].

To assess the impact of sulphite on anaerobic growth of these strains, 10 mL cultures were initially grown overnight in aerobic LB medium (10 g of tryptone, 10 g of NaCl and 5 g of yeast extract per liter, pH 7.0). These cultures were used to inoculate sealed Hungate Tubes containing 14 mL of minimal salts (MS) medium supplemented with 1% LB, 10 μM selenate and 10 μM molybdate with the complete medium brought to pH 6.4 with phosphate [32]. In this medium the main carbon source was 43 mM glycerol and the terminal electron acceptors were 2 mM sodium nitrate and 40 mM sodium fumarate. After 6 hrs growth the cultures were used to inoculate 14 mL of nitrogen flushed MS media in sealed Hungate Tubes. These anaerobic cultures were grown to an absorbance of ca. 0.15 at 600 nm and 140 μL of either 250 mM aqueous Na_2SO_3 (pH 6.4) or water added as desired. Bacteria were grown at 37°C and kanamycin (25 μg mL^{-1}) was added where appropriate.

RESULTS

Sulphite inhibition of NrfA nitrite reduction

The low rates reported for NrfA sulphite reduction when compared to those for nitrite reduction, taken together with crystallographic resolution of these molecules as distal ligands to the active site heme of *W. succinogenes* NrfA, suggested that sulphite would inhibit NrfA nitrite reduction [7, 13, 14, 33]. Previously, PFV was used to resolve inhibition of NrfA nitrite reduction by ions such as cyanide, azide, sulphate and

nitrate, across the electrochemical potential domain, i.e., as a function of enzyme oxidation state [34]. Consequently, PFV was used to assess the impact of sulphite on steady-state nitrite reduction by NrfA (Figure 1A). A 'film' of electrocatalytically active NrfA was adsorbed on an electrode surface and placed in 5 μM nitrite. Cyclic voltammetry revealed a negatively signed catalytic current below ca. -0.1 V that quantified the rate at which electrons moved from the electrode to nitrite via NrfA and as a function of the potential applied to the electrode. The magnitude of the catalytic wave decreased on addition of sulphite but the original magnitude was restored when the film was returned to a solution containing 5 μM nitrite but no sulphite. Thus, sulphite acted as a reversible inhibitor of NrfA nitrite reduction.

In an attempt to identify a catalytic response describing sulphite reduction PFV was also performed in 1 mM sulphite (Figure 1B). Although catalysis was clearly displayed when the film was subsequently transferred to 10 μM nitrite, there was no indication of a catalytic response arising from sulphite reduction by NrfA since the currents below ca. -0.4 V could be attributed to direct reduction of sulphite by the electrode. This result was consistent with sulphite reduction occurring at a rate significantly less than that for nitrite reduction, see below. While this precluded analysis of sulphite reduction by PFV it had the benefit of allowing sulphite to be considered simply as an inhibitor of nitrite reduction such that its interactions with NrfA could be readily quantified as described below.

Sulphite inhibition of NrfA catalysis in 5 μM nitrite was described by IC_{50} values of ca. 150 and 350 μM at -0.25 and -0.60 V, respectively (Figure 1A). Thus, the potency of sulphite as an inhibitor of NrfA was dependent on applied potential and hence the effective oxidation state of the enzyme. To gain greater insight into this behaviour, values for K_M and the maximum catalytic current, i_{max}, (equivalent to V_{max}) were determined as a function of sulphite concentration at these two potentials. For simplicity we relate the behaviours displayed by NrfA poised at -0.25 V and -0.60 V to semi-reduced (SR) and reduced (R) states of NrfA, respectively, given that the catalytic current magnitude is independent of potential below ca. -0.50 V and thus presumably arises from fully reduced enzyme. When NrfA was poised at -0.25 V sulphite had negligible effect on i_{max} but increased K_M in a manner consistent with competitive inhibition with a dissociation constant for sulphite binding to semi-reduced NrfA, K_d^{SR}, of ca. 145 ± 50 μM, circles in (Figure 2 A,B).

For NrfA poised at -0.60 V the presence of sulphite decreased i_{max} and increased K_M indicating a form of mixed-inhibition (Figure 2 A,B). Plots of $1/i_{max}$ and K_M/i_{max} versus sulphite concentration showed hyperbolic- and linear-behaviour, respectively (Figure 2 C,D). This is consistent with formation of a dead-end complex when sulphite binds to reduced NrfA but an active complex when sulphite binds to nitrite-bound reduced NrfA. From the plot of $1/i_{max}$ versus sulphite concentration the dissociation constants describing inhibitor binding to reduced NrfA, K_d^R, and its nitrite complex, $K_d^{R:Nitrite}$, were found to be 178 ± 50 μM and 389 ± 50 μM respectively [17]. These results are summarized in Figure 3.

Spectroscopic studies of sulphite binding to oxidised NrfA

Spectroscopically, the various hemes of oxidised, i.e., all ferric NrfA, are most readily distinguished by X-band electron paramagnetic resonance (EPR) spectroscopy in the perpendicular mode [4]. The four *bis*-histidine coordinated hemes of NrfA are low-spin ($S = ½$). The lysine coordinated heme of the active site is high-spin ($S = {}^5/_2$) where it exists as a mixed population with distal ligation from water and hydroxide. Weak spin-coupling between the high-spin ferric heme and its neighbouring *bis*-histidine coordinated ferric heme results in two prominent features in the perpendicular mode X-band EPR spectrum of oxidised NrfA at 10 K (Figure 4A). These features, a high-field peak with $g \sim 10.8$ and a mid-field derivative having a peak at $g \sim 3.5$ and a relatively broad trough between ca. $g \sim 3.1$ and 2.5, diminish in intensity and change shape when sulphite is titrated into the sample. The high-field peak and mid-field derivative were retained when further additions of sulphite to the sample produced no further changes to the spectrum. Thus, sulphite-bound NrfA contains a weakly spin-coupled pair of high- and low-spin ferric hemes but with the environment around at least one of these hemes distinct from that in oxidised NrfA.

A complementary perspective of heme coordination- and spin-state in sulphite-bound NrfA was provided by room-temperature magnetic circular dichroism (MCD) spectroscopy (Figure 4B). High-spin ferric hemes give rise to charge transfer bands between 600 and 700 nm whose position is indicative of the chemical nature of the axial ligands. Sulphite-bound NrfA displayed a single charge transfer band with a trough at 633

nm. This band was of comparable intensity and position to that displayed by oxidised NrfA in the absence of sulphite and where troughs at 620 and 635 nm reflect overlap of two charge transfer bands corresponding to populations of lysine-hydroxide and lysine-water coordinated high-spin heme respectively [4, 35].

There were no changes in the EPR or MCD spectra on sulphite binding to oxidised NrfA that would indicate changes of heme oxidation- or spin-state. In the MCD spectrum the region below 600 nm that is dominated by contributions from low-spin ferric heme was essentially unchanged by the presence of sulphite. There was no indication of sharp and relatively intense features in the α-/β- region (500 to 550 nm) that would indicate the formation of low-spin ferrous heme or a trough at 600 nm indicative of high-spin ferrous heme. In the EPR spectra, the sharp features at $g \sim 3.1$ and 2.7 that arise from low-spin ferric hemes, either as large g_{max} or spin-coupled features, are not changed by the presence of sulphite. Similarly, sulphite had no impact on the rhombic trio of features at $g \sim 2.9$, 2.3 and 1.5 which arise from a single *bis*-histidine coordinated low-spin ferric heme. Consequently, the changes seen in the EPR monitored titration of sulphite into oxidised NrfA can be attributed simply to sulphite binding to the oxidised enzyme and perturbing the environment of the active site heme. The variation of $g = 3.53$ signal intensity with sulphite concentration is well-described by reversible one-to-one binding of sulphite to oxidised NrfA with a dissociation constant, K_d^O, of 53 ± 20 μM (Figure 4A).

The electronic absorbance spectrum of oxidised NrfA is dominated by contributions from the four low-spin ferric hemes which makes it less sensitive than EPR and MCD to changes at the high-spin ferric heme. Nevertheless there were changes in the electronic absorbance, consistent with the results from EPR and MCD spectroscopy, when sulphite was titrated into oxidised NrfA (supplemental Figure S2). Changes in the Soret region, highlighted in the sulphite-bound minus oxidised NrfA difference spectrum that had a trough at 408 nm, an isosbestic point at 423 nm and peak at 430.5 nm, were consistent with an altered environment of the high-spin ferric heme. In addition, the absorbance at 430.5 nm varied with sulphite concentration in the manner expected for reversible binding of a single molecule of sulphite to a single NrfA subunit with K_d^O = 25 ± 20 μM and in acceptable agreement with the EPR data given the distinct features and errors associated with each type of experiment. The presence of sulphite did not induce changes in the α-/β- region ruling out the formation of low-spin ferrous, or ferric, heme.

Crystallographic resolution of sulphite binding to reduced NrfA

Molecular resolution of the site of sulphite binding to reduced *E. coli* NrfA was afforded by crystals of NrfA that had been soaked with 50 mM $Na_2S_2O_5$ prior to harvesting and that diffracted X-rays to 2.3 Å. Microspectrophotometry established that exposure to X-rays was accompanied by relatively rapid photo-reduction of the NrfA hemes (supplemental Figure S1). This reduction appeared complete within 100 s X-ray exposure. Consequently, to avoid combining data from both oxidised and reduced states of NrfA, only those diffraction images collected after 100 s of cumulative X-ray exposure, i.e., those arising from reduced NrfA, were processed. Refinement using this data showed that the majority of electron density overlaid that resolved from native crystals, i.e., those prepared in the absence of inhibitors and substrates. However, significant additional electron density was observed in the active site of each of the four NrfA monomers within the unit cell. This electron density could be attributed to SO_3^{2-}(HSO_3^-) positioned with the sulphur bound to the iron of the lysine-coordinated heme at a distance of 2.35 ± 0.1 Å, one oxygen H-bonded to Arg106, another oxygen H-bonded to both His264 and Tyr126, and the third oxygen coordinated by a conserved water molecule that was in turn H-bonded to the propionate groups of the lysine-coordinated heme (supplemental Fig. S3). This was the only orientation of SO_3^{2-} that could provide a satisfactory fit to the electron density and it was similar to that reported for SO_3^{2-}(HSO_3^-) bound to *W. succinogenes* NrfA. The average temperature factors (B-factor) of the active site sulphite molecules were similar to the average B-factors of the other ligands (Supplemental Table S1), indicating that the electron density at the active site could be adequately attributed to the presence of SO_3^{2-} (HSO_3^-). Additional electron density was also identified on the surface of one NrfA subunit and this could be attributed to a fifth ion in the unit cell coordinated via the side-chains of Lys322 and the backbone amide groups of Phe310 and Ala311. However, the significance of this finding is unclear since it may arise from adventitious association of SO_3^{2-} (HSO_3^-) to the surface of NrfA under the conditions of co-crystal formation. When the positions of the main chain atoms from the 1.7 Å resolution structure of the native *E. coli* NrfA monomer were superposed with atoms in the

corresponding 2.3 Å resolution structure of the SO_3^{2-}(HSO_3^-) bound NrfA monomer, the overall root mean square deviation was 0.483 Å. This indicates that SO_3^{2-}(HSO_3^-) binds to NrfA without causing significant conformational changes.

The sulphite reductase activity of NrfA

Steady-state analysis of NrfA sulphite reduction was performed using a spectrophotometric assay with zinc reduced methyl viologen as the electron donor. The results were well described by the Michaelis-Menten equation with K_M = 70 ± 15 μM and k_{cat} = 0.03 ± 0.005 molecules of sulphite reduced s^{-1} giving a specificity constant (k_{cat}/K_M) of the order of 4.3×10^3 M^{-1} s^{-1} (Figure 5). In the same assay, nitrite reduction by NrfA was described by K_M = 22 ± 7 μM, k_{cat} = 769 ± 20 molecules of nitrite reduced s^{-1} and k_{cat}/K_M of the order of 3.5×10^7 M^{-1} s^{-1}. To verify the product of sulphite reduction, NrfA (3 μM) was incubated anaerobically with dithionite (10 μM) as the source of sulphite and electrons; $S_2O_4^{2-} + 2H_2O \rightarrow 2HSO_3^- + 2H^+ + 2e^-$. Dithionite oxidation occurred at a rate of 0.8 ± 0.05 electrons s^{-1} and sulphide was formed at a rate of 0.14 ± 0.1 molecules s^{-1}. The ratio of these rates is 5.7 ± 2 consistent with the six-electron reduction of sulphite to sulphide.

Impact of *nrfA* deletion on anaerobic growth in the presence of sulphite

Anaerobic growth of the *E. coli nrfA* deletion strain and the parent strain, DH10B, were compared in the presence and absence of sulphite to assess whether NrfA conferred resistance to sulphite (Figure 6). A pulse of 35 μmol sulphite was added to both cultures during early exponential growth with nitrate and fumarate as the terminal electron acceptors and glycerol as the non-fermentable carbon source. Growth of both strains was arrested by the addition of sulphite (Figure 6A). However, while the parent strain resumed growth after ca. 12 hrs the growth of the *nrfA* deletion strain was arrested for at least 20 hrs. The ability of NrfA to confer resistance to sulphite was confirmed in control experiments where water, of equal volume to that containing 35 μmol sulphite, was added to the cultures (Figure 6B). Both strains reached stationary phase within ca. 12 hrs with the *nrfA* deletion strain having a slightly lower final optical density than the parent strain.

DISCUSSION

The ability of NrfA to reduce sulphite to sulphide has been known for some time [3, 7, 13, 14]. However, the possible cellular consequences of this activity have received little attention. For *E. coli* NrfA, a periplasmic enzyme in an enteric pathogen, exogenous sulphite may be encountered in various contexts during colonisation of a human host. Sulphite can be encountered in the gastrointestinal tract since it is added to certain foods and beverages as an antimicrobial [15]. *E. coli* that enters the blood stream as a prelude to sepsis or meningitis may also encounter sulphite since it is produced by neutrophils as part of host defence against microbial invasion [16]. Consequently, the dissociation constants and kinetic parameters presented here provide not only a quantitative description of interactions between a redox enzyme and its substrate but a biochemical framework from which to consider the cellular consequences of the interactions between sulphite and the wide-spread multi-heme cytochrome NrfA.

Resolution of dissociation constants describing the affinity of a substrate for multiple oxidation states of an oxidoreductase is relatively rare. Substrate binding to a catalytically competent oxidation state is typically followed by relatively rapid events leading to product formation and that preclude isolation of the binding event. Here the interactions of sulphite with catalytically competent semi-reduced and fully-reduced NrfA were resolved by taking advantage of the relatively low rate of sulphite, as compared to nitrite, reduction. This allowed well-established models of enzyme inhibition to provide dissociation constants for various redox states of NrfA as defined by the potential applied to the electrode in the PFV experiments. For both fully- and semi-reduced NrfA there was competition between sulphite and nitrite for binding to the active site. This is a finding that is consistent with both SO_3^{2-} (HSO_3^-) and nitrite being substrates for NrfA and the resolution of both of these molecules as distal ligands to the active site heme in crystals of oxidised *W. succinogenes* NrfA [13]. Crystals of reduced *E. coli* NrfA coordinate SO_3^{2-} (HSO_3^-) in a manner indistinguishable from that in the *W. succinogenes* enzyme and as expected from the extensive homology between these enzymes. That crystals of *E. coli* NrfA contain reduced, catalytically competent enzyme may be explained by a turnover number that at the cryogenic temperatures of the X-ray diffraction must be

significantly lower than that of 0.03 sulphite molecules reduced s^{-1} at room temperature. However, other interpretations cannot be excluded. It may be that SO_2, present in equilibrium with the anionic forms SO_3^{2-} (HSO_3^-) in aqueous solution, is the true substrate of NrfA and that the anionic forms bind preferentially under the conditions of crystallization. Equally it may be that the crystallized forms do not lie on the catalytic pathway as has been observed for other enzymes with relatively small anionic substrates [36].

In this study information on sulphite binding to solutions of *E. coli* NrfA was provided by optical spectroscopies and complemented by information on frozen solutions afforded by EPR spectroscopy. Each of these spectroscopies indicated that sulphite bound to oxidised NrfA at, or in close proximity to, the high-spin lysine coordinated ferric heme of the active site. It is less certain that binding reflects sulphur ligation of the ferric heme as found in the co-crystals. Both EPR and optical spectroscopies showed that the active site heme remains high-spin ferric when sulphite is bound to NrfA. The MCD between 600 and 700 nm of as-prepared and sulphite-bound NrfA are very similar. This region of the spectrum is diagnostic of the chemical nature of the ligands to high-spin ferric heme and the troughs that are observed from as-isolated NrfA are consistent with a mixed population of hemes with lys-hydroxide and lys-water ligation in line with crystal structure [4]. We have not been able to find literature precedent for spectroscopic characterisation of a high-spin ferric c-, or b-, heme with axial ligation from nitrogen and sulphur. However, a discernable change in the MCD spectrum between 600 and 700 nm is expected if sulphur replaces oxygen as a heme ligand to give axial coordination as resolved by the crystal structure. Instead, the spectra are more readily explained by retention of nitrogen and oxygen ligation. This may arise from a small displacement of the overlapping derivatives from lysine-hydroxide and lysine-water coordinated hemes if sulphite binds in the vicinity of the active site leaving water/hydroxide as axial ligand(s). Alternatively sulphite may bind the active site heme through an oxygen atom. In either case, reduction of NrfA must be accompanied by reorganisation within the active site if sulphur ligation of the active site heme is a requirement for sulphite reduction.

The affinity of the active site for sulphite decreases on reduction of NrfA as summarised in Figure 3. However, the decrease is minor when compared to that for other anions [34]. Thiocyanate, nitrate and azide bind oxidised NrfA with dissociation constants of the order of 42, 73 and 38 μM, respectively, and that are comparable to that of 54 μM for sulphite. On reduction of NrfA the affinities for thiocyanate, nitrate and azide drop 50-, 140- and 380-fold whereas that for sulphite drops only 3-fold. Thus, it appears that NrfA has a mechanism to retain sulphite within its active site when it accumulates the reducing equivalents needed for reduction of this molecule. This mechanism may be reflected in the changes of coordination within the active site described above and that presumably contrast to the modes of binding thiocyanate, nitrate and azide. The K_M for sulphite reduction of ca. 70 μM is comparable to the dissociation constants describing sulphite binding to the active site of NrfA in its oxidised, semi-reduced and reduced states. Consequently, the K_M is effectively a measure of the affinity of sulphite for the active site and the same is likely to be true for the other NrfA substrates, nitrite and nitric oxide for which the K_M values are 30 and 300 μM respectively under comparable conditions [8]. Thus, sulphite may well compete effectively with nitric oxide and also nitrite for binding to *E. coli* NrfA *in vivo* for example in blood plasma where the concentration of sulphite may rise to 30 μM and exceed that of nitrite at ca. 1 μM [37, 38]. Assessing the impact of exogenous sulphite on rates of nitrite respiration and nitric oxide detoxification was beyond the scope of these studies. However, the finding that NrfA confers resistance to exogenous sulphite during anaerobic growth of *E. coli* demonstrates that interactions between NrfA and sulphite are possible in the cellular context. It is likely that the sulphite reductase activity of NrfA, rather than a capability to sequester sulphite, underpins this finding since growth of *E. coli* is restored after several hours incubation with sulphite that may be detoxified through its removal from the culture by precipitation as an inorganic sulphide or conversion to the volatile gas hydrogen sulphide.

In closing we note that bioinformatic and structural studies have shown the NrfA enzymes to be highly homologous [1]. Many of the amino acid residues defining not only the active sites but also the channels linking these sites to the protein surfaces are identical. Thus, the quantitative descriptions of the interactions between sulphite and the active site of *E. coli* NrfA presented here should prove to be applicable to many, if not all, members of the NrfA family. It is difficult to predict whether the second site for sulphite binding to *E. coli* NrfA, as revealed by mixed-inhibition of nitrite reduction at low potentials, will be found in other members of the enzyme family. We were unable to provide unambiguous resolution of this secondary sulphite-binding site, although crystallographic resolution of sulphite bound to the surface of reduced NrfA near a low potential his-his coordinated heme is one possibility. It is hoped that in the future PFV of NrfA enzyme from other organisms and/or site-specific engineering of *E. coli* NrfA will resolve this. For the

moment it is worth noting that the catalytic wave describing reduction of 5 μM nitrite changes from a peaked response to one containing two sigmoidal increases of activity as sulphite is titrated into the experiment. The same change of wave-shape is seen when nitrite is titrated into such an experiment, although accompanied by an increase rather than a decrease in the magnitude of the response (supplemental Figure S4) [12]. These similarities may arise because nitrite, in addition to sulphite, can bind to the site on NrfA that is revealed on full-reduction of the enzyme.

FUNDING
The UK Biotechnology and Biological Sciences Research Council [C007808, B18695 and G009228] and a PhD studentship to G.L.K.

REFERENCES

1 Simon, J. (2002) Enzymology and bioenergetics of respiratory nitrite ammonification. FEMS Microbiol. Rev. **26**, 285-309

2 Einsle, O., Messerschmidt, A., Stach, P., Bourenkov, G. P., Bartunik, H. D., Huber, R. and Kroneck, P. M. H. (1999) Structure of cytochrome *c* nitrite reductase. Nature. **400**, 476-480

3 Einsle, O., Stach, P., Messerschmidt, A., Simon, J., Kroger, A., Huber, R. and Kroneck, P. M. H. (2000) Cytochrome *c* nitrite reductase from *Wolinella succinogenes* - Structure at 1.6 angstrom resolution, inhibitor binding, and heme-packing motifs. J. Biol. Chem. **275**, 39608-39616

4 Bamford, V. A., Angove, H. C., Seward, H. E., Thomson, A. J., Cole, J. A., Butt, J. N., Hemmings, A. M. and Richardson, D. J. (2002) Structure and spectroscopy of the periplasmic cytochrome *c* nitrite reductase from *Escherichia coli*. Biochemistry. **41**, 2921-2931

5 Cunha, C. A., Macieira, S., Dias, J. M., Almeida, G., Goncalves, L. L., Costa, C., Lampreia, J., Huber, R., Moura, J. J. G., Moura, I. and Romao, M. J. (2003) Cytochrome *c* nitrite reductase from *Desulfovibrio desulfuricans* ATCC 27774 - The relevance of the two calcium sites in the structure of the catalytic subunit (NrfA). J. Biol. Chem. **278**, 17455-17465

6 Einsle, O., Messerschmidt, A., Huber, R., Kroneck, P. M. H. and Neese, F. (2002) Mechanism of the six-electron reduction of nitrite to ammonia by cytochrome *c* nitrite reductase. J. Am. Chem. Soc. **124**, 11737-11745

7 Stach, P., Einsle, O., Schumacher, W., Kurun, E. and Kroneck, P. M. H. (2000) Bacterial cytochrome *c* nitrite reductase: new structural and functional aspects. J. Inorg. Biochem. **79**, 381-385

8 van Wonderen, J. H., Burlat, B., Richardson, D. J., Cheesman, M. R. and Butt, J. N. (2008) The nitric oxide reductase activity of cytochrome *c* nitrite reductase from *Escherichia coli*. J. Biol. Chem. **283**, 9587-9594

9 Costa, C., Macedo, A., Moura, I., Moura, J. J. G., Legall, J., Berlier, Y., Liu, M. Y. and Payne, W. J. (1990) Regulation of the hexaheme nitrite nitric-oxide reductase of *Desulfovibrio desulfuricans*, *Wolinella succinogenes* and *Escherichia coli* - a mass-spectrometrc study. FEBS Letters. **276**, 67-70

10 Poock, S. R., Leach, E. R., Moir, J. W. B., Cole, J. A. and Richardson, D. J. (2002) Respiratory detoxification of nitric oxide by the cytochrome *c* nitrite reductase of *Escherichia coli*. J. Biol. Chem. **277**, 23664-23669

11 Mills, P. C., Rowley, G., Spiro, S., Hinton, J. C. D. and Richardson, D. J. (2008) A combination of cytochrome *c* nitrite reductase (NrfA) and flavorubredoxin (NorV) protects *Salmonella enterica serovar* Typhimurium against killing by NO in anoxic environments. Microbiology-SGM. **154**, 1218-1228

12 Angove, H. C., Cole, J. A., Richardson, D. J. and Butt, J. N. (2002) Protein film voltammetry reveals distinctive fingerprints of nitrite and hydroxylamine reduction by a cytochrome *c* nitrite reductase. J. Biol. Chem. **277**, 23374-23381

13 Lukat, P., Rudolf, M., Stach, P., Messerschmidt, A., Kroneck, P. M. H., Simon, J. and Einsle, O. (2008) Binding and reduction of sulfite by cytochrome *c* nitrite reductase. Biochemistry. **47**, 2080-2086

14 Clarke, T. A., Hemmings, A. M., Burlat, B., Butt, J. N., Cole, J. A. and Richardson, D. J. (2006) Comparison of the structural and kinetic properties of the cytochrome *c* nitrite reductases from *Escherichia coli*, *Wolinella succinogenes*, *Sulfurospirillum deleyianum* and *Desulfovibrio desulfuricans*. Biochem. Soc. Trans. **34**, 143-145

15 Taylor, S., Highley, N. and Bush, R. (1986) Adv. Food. Res. **30**, 1-76

16 Mitsuhashi, H., Nojima, Y., Tanaka, T., Ueki, K., Maezawa, A., Yano, S. and Naruse, T. (1998) Sulfite is released by human neutrophils in response to stimulation with lipopolysaccharide. J. Leukoc. Biol. **64**, 595-599
17 Clarke, T. A., Mills, P. C., Poock, S. R., Butt, J. N., Cheesman, M. R., Cole, J. A., Hinton, J. C. D., Hemmings, A. M., Kemp, G., Soderberg, C. A. G., Spiro, S., Van Wonderen, J. and Richardson, D. J. (2008) *Escherichia coli* cytochrome *c* nitrite reductase NrfA. Meth. Enzymol. **437**, 63-77
18 Gwyer, J. D., Richardson, D. J. and Butt, J. N. (2005) Diode or tunnel-diode characteristics? Resolving the catalytic consequences of proton coupled electron transfer in a multi-centered oxidoreductase. J. Am. Chem. Soc. **127**, 14964-14965
19 Cleland, W. W. (1970) The Enzymes, Kinetics and Mechanism. Academic Press, New York
20 Leslie, A. G. W. (1999) Integration of macromolecular diffraction data. Acta Cryst. D. **55**, 1696-1702
21 Evans, P. (2006) Scaling and assessment of data quality. Acta Cryst. D. **62**, 72-82
22 Collaborative Computational Project, N. (1994) Acta Cryst. D. **62**, 72-82
23 Clarke, T. A., Kemp, G. L., Van Wonderen, J. H., Doyle, R., Cole, J. A., Tovell, N., Cheesman, M. R., Butt, J. N., Richardson, D. J. and Hemmings, A. M. (2008) Role of a conserved glutamine residue in tuning the catalytic activity of *Escherichia coli* cytochrome *c* nitrite reductase. Biochemistry. **47**, 3789-3799
24 Emsley, P. and Cowtan, K. (2004) Coot: model-building tools for molecular graphics. Acta Cryst. D. **60**, 2126-2132
25 Murshudov, G. N., Vagin, A. A. and Dodson, E. J. (1997) Refinement of macromolecular structures by the maximum-likelihood method. Acta Cryst. D. **53**, 240-255
26 Cohen, S. X., Morris, R. J., Fernandez, F. J., Ben Jelloul, M., Kakaris, M., Parthasarathy, V., Lamzin, V. S., Kleywegt, G. J. and Perrakis, A. (2004) Towards complete validated models in the next generation of ARP/wARP. Acta Cryst. D. **60**, 2222-2229
27 Davis, I. W., Leaver-Fay, A., Chen, V. B., Block, J. N., Kapral, G. J., Wang, X., Murray, L. W., Arendall, W. B., Snoeyink, J., Richardson, J. S. and Richardson, D. C. (2007) MolProbity: all-atom contacts and structure validation for proteins and nucleic acids. Nucleic Acids Research. **35**, W375-W383
28 Mayhew, S. G. (1978) Redox potential of dithionite and SO_2^- from equilibrium reactions with flavodoxins, methyl viologen and hydrogen plus hydrogenase. Eur. J. Biochem. **85**, 535-547
29 Cline, J. D. (1969) Spectrophotometric determination of hydrogen sulfide in natural waters. Limnol. Oceanogr. **14**, 454-458
30 Datsenko, K. A. and Wanner, B. L. (2000) One-step inactivation of chromosomal genes in *Escherichia coli* K-12 using PCR products. Proc. Nat. Acad. Sci. U.S.A. **97**, 6640-6645
31 Poock, S. R. (2004) PhD Thesis. ed.)^eds.), University of East Anglia
32 Pope, N. R. and Cole, J. A. (1984) Pyruvate and ethanol as electron donors for nitrite reduction by *Escherichia coli* K12. J. Gen. Microbiol. **130**, 1279-1284
33 Pereira, I. C., Abreu, I. A., Xavier, A. V., LeGall, J. and Teixeira, M. (1996) Nitrite reductase from *Desulfovibrio desulfuricans* (ATCC 27774) - A heterooligomer heme protein with sulfite reductase activity. Biochem. Biophys. Res. Comm. **224**, 611-618
34 Gwyer, J. D., Richardson, D. J. and Butt, J. N. (2006) Inhibiting *Escherichia coli* cytochrome *c* nitrite reductase: voltammetry reveals an enzyme equipped for action despite the chemical challenges it may face in vivo. Biochem. Soc. Trans. **34**, 133-135
35 Burlat, B., Gwyer, J. D., Poock, S., Clarke, T., Cole, J. A., Hemmings, A. M., Cheesman, M. R., Butt, J. N. and Richardson, D. J. (2005) Cytochrome *c* nitrite reductase: from structural to physicochemical analysis. Biochem. Soc. Trans. **33**, 137-140
36 Zajicek, R. S., Cheesman, M. R., Gordon, E. H. J. and Ferguson, S. J. (2005) Y25S variant of *Paracoccus pantotrophus* cytochrome cd_1 provides insight into anion binding by d_1 heme and a

rare example of a critical difference between solution and crystal structures. Journal of Biological Chemistry. **280**, 26073-26079

37 Farrell, A. J., Blake, D. R., Palmer, R. M. J. and Moncada, S. (1992) Increased concentrations of nitrite in synovial-fluid and serum samples suggest increased nitric-oxide synthesis in rheumatic disease. . Ann. Rheum. Dis. **51**, 1219-1222

38 Jin, H. F., Du, S. X., Zhao, X., Wei, H. L., Wang, Y. F., Liang, Y. F., Tang, C. S. and Du, J. B. (2008) Effects of endogenous sulfur dioxide on monocrotaline-induced pulmonary hypertension in rats. Acta Pharmacol. Sin. **29**, 1157-1166

FIGURE LEGENDS

Figure 1 PFV of *E. coli* NrfA in the presence of sulphite and/or nitrite

(A) Baseline subtracted steady-state voltammetry from a NrfA film in 5 μM nitrite with 0, 20, 100, 200, 500 or 1000 μM sulphite as indicated. (B) Baseline subtracted voltammetry from a NrfA film in 1 mM sulphite (heavy solid line) and after transfer to 10 μM nitrite (light solid line). The catalytic response from a freshly polished electrode placed in 1 mM sulphite (broken line). Buffer-electrolyte 50 mM Hepes, 2 mM $CaCl_2$, pH 7.0, 20 °C with a scan rate of 30 mV s^{-1} and electrode rotation at 3000 rpm.

Figure 2 Summary of kinetic parameters for *E. coli* NrfA nitrite reduction in the presence of sulphite

Data from PFV with the NrfA film poised at -0.25 V (circles) or -0.6 V (squares) and experimental conditions as in Fig. 3. The lines represent best fits to the data as described in the text; in (B) K_d^{SR} = 145 μM and in (C) K_d^{R} = 178 μM and $K_d^{R:Nitrite}$ = 389 μM. In (D) the line shows the best linear fit to the data.

Figure 3 Summary of thermodynamic parameters describing sulphite binding to *E. coli* NrfA

The square represents NrfA in different oxidation states; oxidised = open square, semi-reduced = half-filled square, reduced = filled square. Dissociation constants for reversible binding of a single sulphite molecule to NrfA were determined for oxidised NrfA (K_d^{O}) from spectroscopic studies, and for semi-reduced (K_d^{SR}) and reduced (K_d^{R}) NrfA from protein film voltammetry defining sulphite inhibition of NrfA nitrite reduction at -0.25 and -0.6 V respectively. See text for details.

Figure 4 EPR and MCD spectroscopy of sulphite equilibrated *E. coli* NrfA

(A) X-band EPR spectra of NrfA (154 μM) equilibrated with 0 (thin solid line), 38.3, 76.1, 150, 617 and 2480 (thick solid line) μM sulphite. Approximate *g*-values indicated in italics. Inset: Intensity change at g = 3.53 as function of sulphite concentration and line showing the behaviour predicted for reversible binding of a single sulphite to NrfA with K_d^{O} = 53 μM. Spectrometer parameters: microwave frequency 9.56 GHz, microwave power 2 mW, modulation amplitude 10 G, temperature 10 K. Spectra have been corrected for the effects of dilution on addition of sulphite. (B) Room temperature MCD of 124 μM NrfA (broken line) and 127 μM NrfA equilibrated with 2480 μM sulphite (solid line). All samples in 50 mM Hepes, 2 mM $CaCl_2$, pH 7.0.

Figure 5 The sulphite reductase activity of *E. coli* NrfA

Rates were measured using zinc reduced methyl viologen as electron donor with 0.3 μM NrfA in 50 mM Hepes, 2 mM $CaCl_2$, 5 mM EDTA, pH 7.0 at room temperature. Line shows best fit to the Michaelis-Menten equation with K_M = 70 μM and V_{max} = 0.029 sulphite molecules reduced s^{-1}. The error bars represent the standard deviation of three assays at each sulphite concentration.

Figure 6 Anaerobic growth of *E. coli* in glycerol/nitrate/fumarate medium in the presence and absence of sulphite.

The absorbance at 600 nm of *E. coli nrfA* (squares) and the parent strain DH10B (circles). Anaerobic solutions containing 35 µmol sulphite (A) or water (B) were added at an absorbance of ca. 0.15 as indicated by the arrows.

Biochemical Journal Immediate Publication. Published on 15 Jul 2010 as manuscript BJ20100866

Figure 1

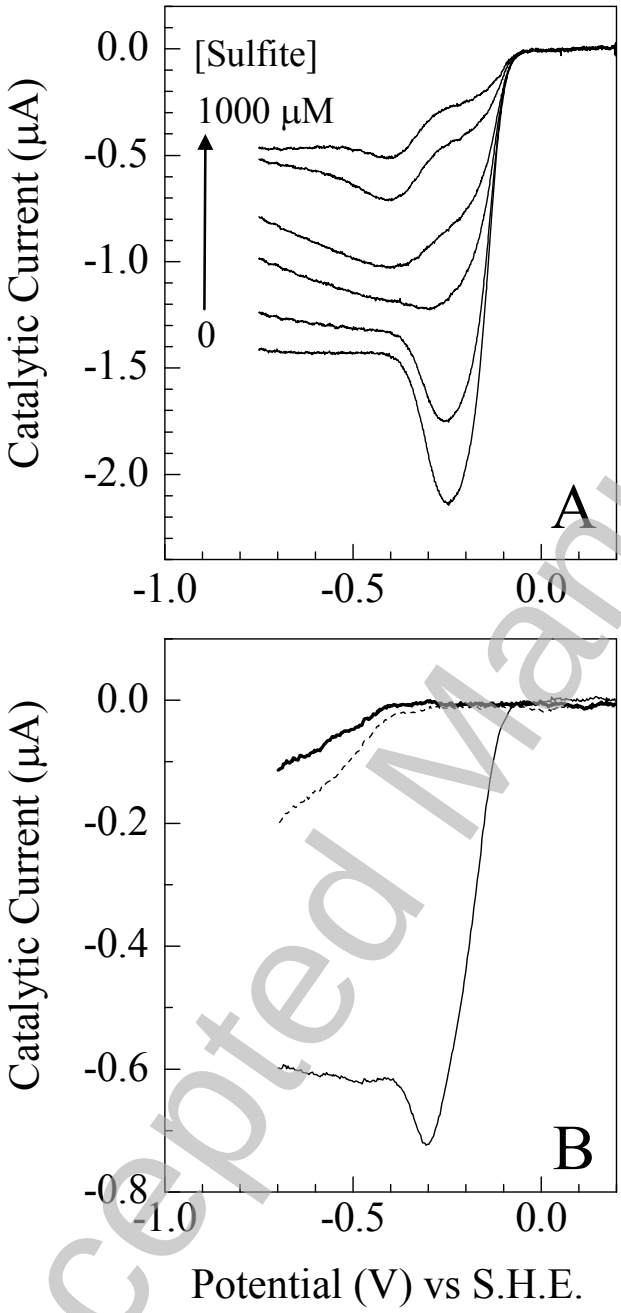

Figure 2

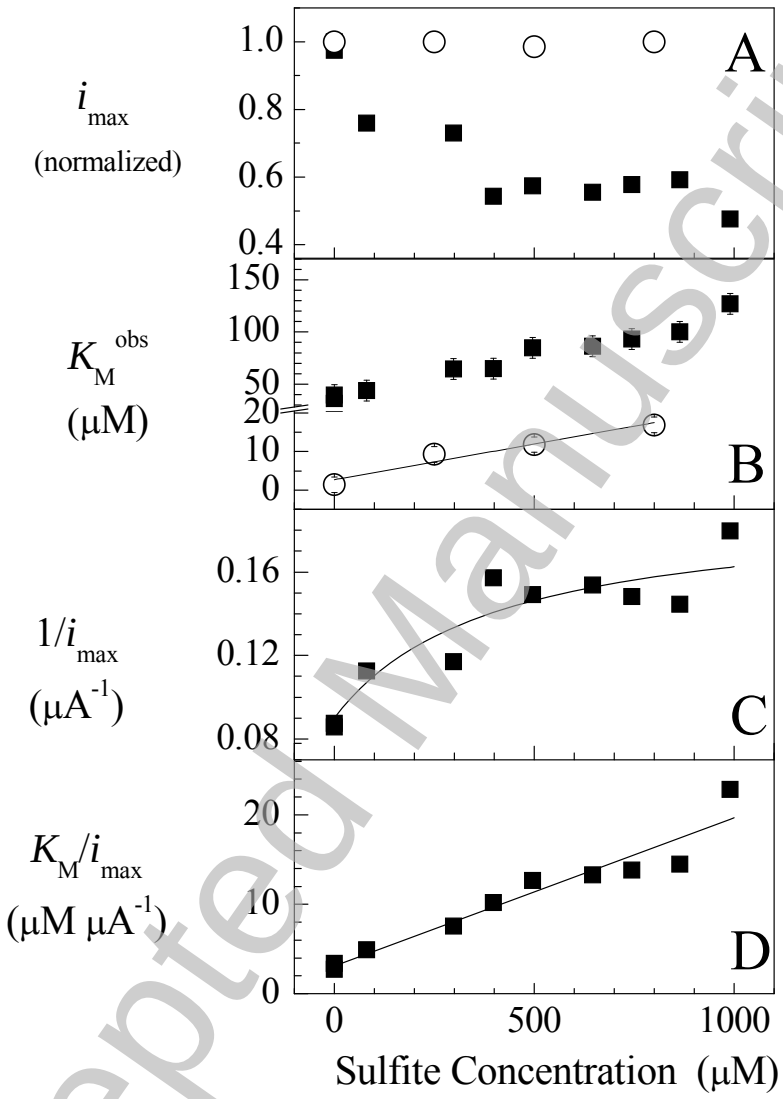

Figure 3

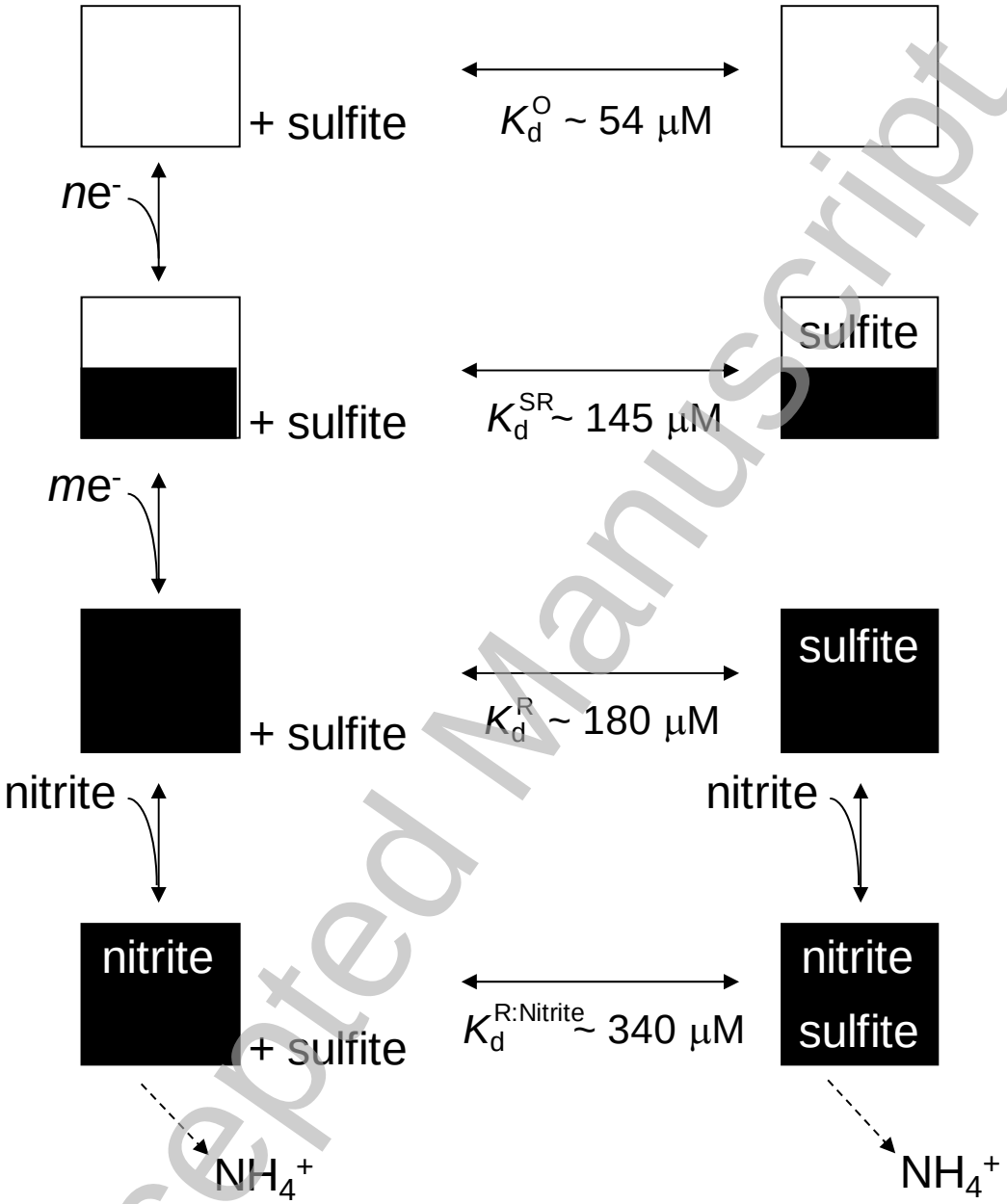

Figure 4

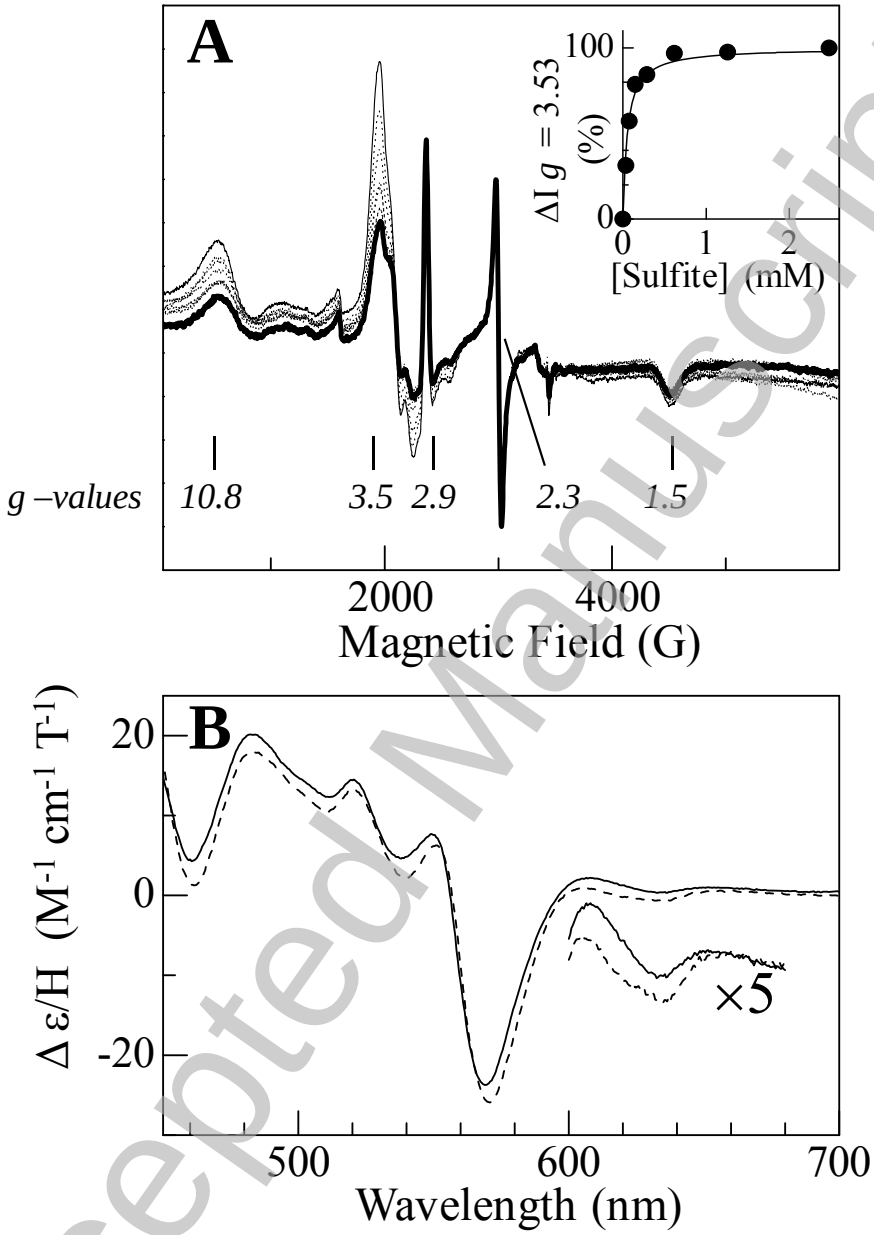

Figure 5

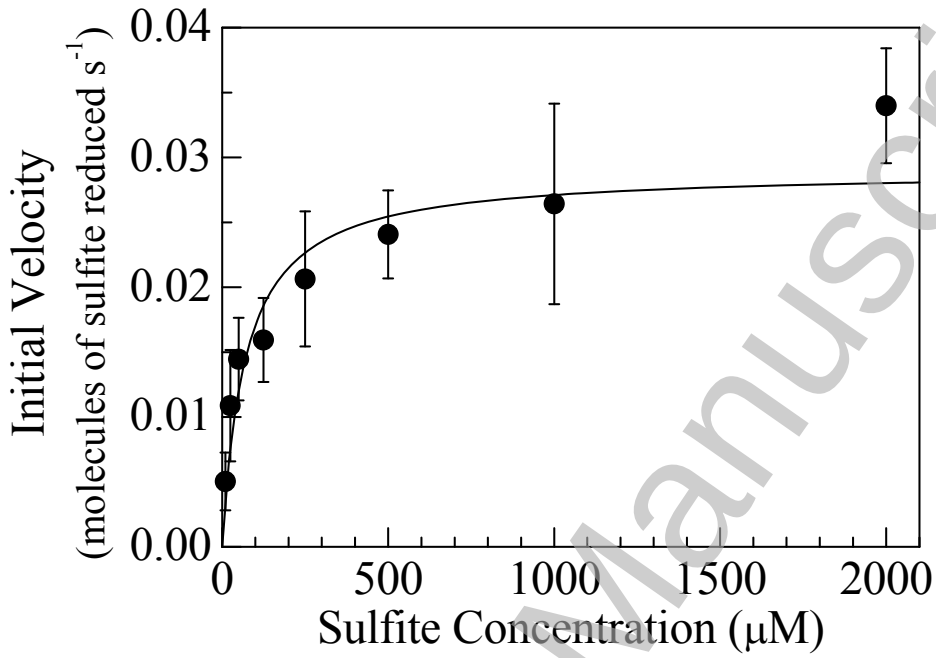

Biochemical Journal Immediate Publication. Published on 15 Jul 2010 as manuscript BJ20100866

Figure 6